IL NUOVO CIMENTO **38 C** (2015) 78
DOI 10.1393/ncc/i2015-15078-1

COMMUNICATIONS: SIF Congress 2014

Mapping the charge carrier density in semiconductors by THz-QCL based optical feedback interferometry

F. P. MEZZAPESA(*)

Dipartimento Interateneo di Fisica, Università degli Studi e Politecnico di Bari - Bari, Italy
CNR-IFN UOS Bari - Bari, Italy

received 30 January 2015

Summary. — A THz imaging system based on self-mixing (SM) interferometry in a Quantum Cascade Laser (QCL) is developed to map the distribution of free charges on a semiconductor surface. In the experiment, a free electron plasma is photo-generated in a high resistivity n-type silicon wafer using a near-infrared (NIR) continuous-wave (CW) pump laser. A model based on Drude theory correctly reproduces the experimental results and in prospective promises a quantitative evaluation of the free charges density.

PACS 42.72.Ai – Infrared sources.
PACS 42.30.-d – Imaging and optical processing.
PACS 42.25.Hz – Interference.

1. – Introduction

When a semiconductor laser is subjected to optical reinjection from an external target (SM configuration) the intracavity laser field coherently interferes with the back reflected radiation carrying information about the target motion and/or its optical proprieties. This leads to a number of applications in metrology and sensing [1]. Coherent imaging that exploits the SM effect in THz QCLs is currently very promising in sensing and material processing applications mostly because of the high CW output power of THz QCLs, coupled with their high sensitivity to optical reinjection and narrow linewidth [2,3]. Moreover, because of the high value of the photon to carrier lifetime ratio ($\approx 10^1$ ps), and to the negligible linewidth enhancement factor ($\alpha \approx 0.5$ [4]), THz QCLs tolerate strong optical feedback levels without exhibiting dynamical instabilities such as mode-hopping, or coherence collapse [5]. Here, these unique features together with the free carriers dependence on the semiconductor dielectric response in the THz frequency range, are exploited

(*) E-mail: francesco.mezzapesa@uniba.it

to demonstrate an innovative technique for imaging free carriers on a semiconductor surface via SM in THz QCLs. In the SM scheme, the coherent superposition of the laser field with the radiation back reflected from the semiconductor target manifests itself as voltage variations across the THz QCL terminals. Hence, the THz QCL acts both as an emitter and a detector of changes in the semiconductor target reflectivity induced by a spatially modulated free carriers density. The Drude theory for free carriers allows to associate the measured SM signal with the corresponding carriers density variation. In the experiment, the latter is induced by photo-excitation with a reconfigurable pattern of a NIR pump. Compared to other optical techniques, such us plasma resonance and free carrier absorption which show better sensitivity and accuracy, or THz near-field nanoscopy and pump and probe microscopy that allow for higher spatial resolution [6-9], the advantage of the proposed THz imaging system consists in being more compact, detector-free and real-time. These features, together with the ultrafast response time of THz QCLs (few picoseconds) yield to conceive future applications such us the direct investigation of the spatiotemporal free carriers distribution in active devices (organic transistors, photovoltaic cells, etc.).

2. – Experimental setup

Figure 1 shows the experimental setup [10], consisting of a CW diode pump laser in the near infrared ($\lambda^{IR} = 832\,\mathrm{nm}$) whose radiation pattern can be riconfigured by a spatial light modulator and illuminates a high resistivity 1 mm thick n-type silicon wafer.

The modulated pattern of photo-excited charges induces a modulation of the silicon target reflectance $R_{\mathrm{ext}} = |E_R/E_I|^2$ that is detected, in the SM configuration, using a probe beam at $\lambda^{\mathrm{THz}} = 76.3\,\mu\mathrm{m}$ (3.93 THz) delivered by a as resonant-phonon single-mode QCL with a surface plasmon waveguide. The SM interference between the intracavity THz field and the reflected THz radiation collected by parabolic mirrors and coupled back into the laser cavity can be detected as voltage modulation across the QCL terminals. For calibration purposes (see next paragraph), the transmitted THz power is also measured by a pyroelectric detector (not shown in the picture) by making use of the ≈ 0.55 transmittance of the THz radiation of the Tydex silicon sample.

3. – Uniform distribution of photo-generated free carriers

In case of uniform target illumination, fig. 2(a) shows the monotonic increase of the THz transmittance $T_{\mathrm{THz}} = |E'_T/E_I|^2$, and the corresponding decrease of the SM signal, with the NIR pump intensity I up to an asymptotic value reached for $I \approx 40\,\mathrm{mW/cm^2}$.

As expected from the Lang-Kobayashi theory of self-mixing in semiconductor lasers [1] that predicts a linear dependence of the interferometric signal on $(R_{\mathrm{ext}})^{1/2}$ (and thus on $(T_{\mathrm{THz}})^{1/2}$), fig. 2(b) shows that the voltage modulation across the QCL terminals is linked to the square root of sample transmittance T_{THz} by a nearly linear relation (R^2 coefficient = 0.9762). Given the sample transmittance dependence from the free carriers as accounted by the Drude model [11] (see next section), the calibration curve in fig. 2(b) allows to correlate the free carriers density with the SM signal.

4. – Drude model for the silicon THz response

Referring to the sketch in the inset of fig. 1, in the hypothesis that a CW pump beam of intensity I normally impinges onto the silicon surface ($z = 0$), by solving the dynamical

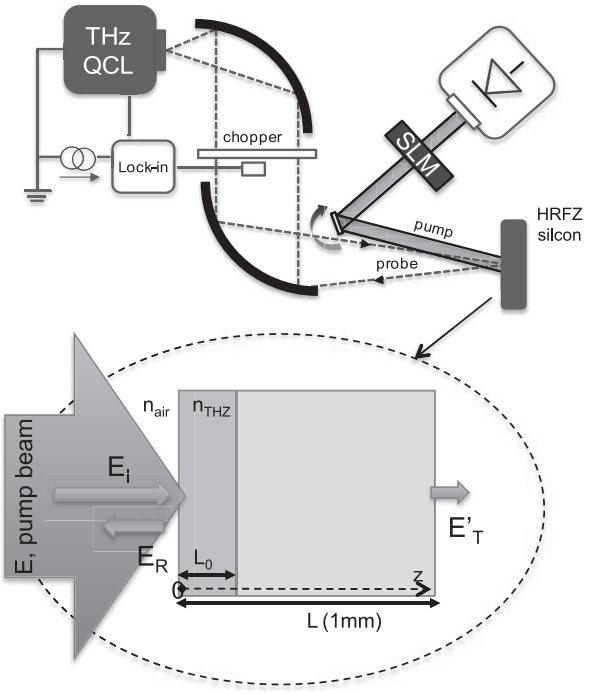

Fig. 1. – Experimental layout. A NIR laser beam ($\lambda^{IR} = 832\,\mathrm{nm}$), pump beam, passing trough a spatial light modulator (SLM) illuminates a high resistivity float zone n-doped (HRFZ) Tydex silicon wafer (`http://www.tydexoptics.com`). In the SM configuration, the spatial distribution of the photo-excited carriers induces a voltage variation at the THz QCL terminals that is detected after amplification via a lock-in amplifier triggered by a mechanical chopper. Inset (not in scale): schematic of the silicon sample of length $L = 1\,\mathrm{mm}$. $L_0 \approx 13\,\mu\mathrm{m}$ is the absoption length at the pump beam wavelenght $\lambda^{IR} = 832\,\mathrm{nm}$ where the density of photo-generated carriers is mainly concentrated. E_I, E_R, E'_T represent the complex envelopes of the incident, reflected and transmitted THz probe beam respectively, and E is the spatially modulated envelope of the pump beam.

equations for the NIR slowly varying envelope of the electric field E ($I = |E|^2 c n^{IR}/2$, where n^{IR} = background refractive index) and the carrier density in the conduction band N, at steady state [12]:

$$N = \frac{N^* + N_0 I/I_{\mathrm{sat}}}{1 + I/I_{\mathrm{sat}}}, \qquad I_{\mathrm{sat}} = \frac{\hbar\omega^{IR}}{A\tau_R} \tag{1}$$

with N^* being the carrier density of the pristine sample and N_0 the carrier density at transparency. In the expression of the saturation intensity I_{sat}, ω^{IR} represents the NIR angular frequency, τ_R the nonradiative carrier decay time (Shockley-Read-Hall recombination), and A is the differential absorption. If the incident THz field is a plane wave with the angular frequency $\omega^{\mathrm{THz}} = ck^{\mathrm{THz}}$, normally impinging onto the semiconductor slab and polarized in the x-y plane (orthogonal to the propagation direction z), namely

$$\mathbf{E}^{\mathrm{THz}}(z,t) = \mathbf{e}\frac{E_I}{2}\exp\left(i(k^{\mathrm{THz}}z - \omega^{\mathrm{THz}}t)\right) + \mathrm{c.c.} \tag{2}$$

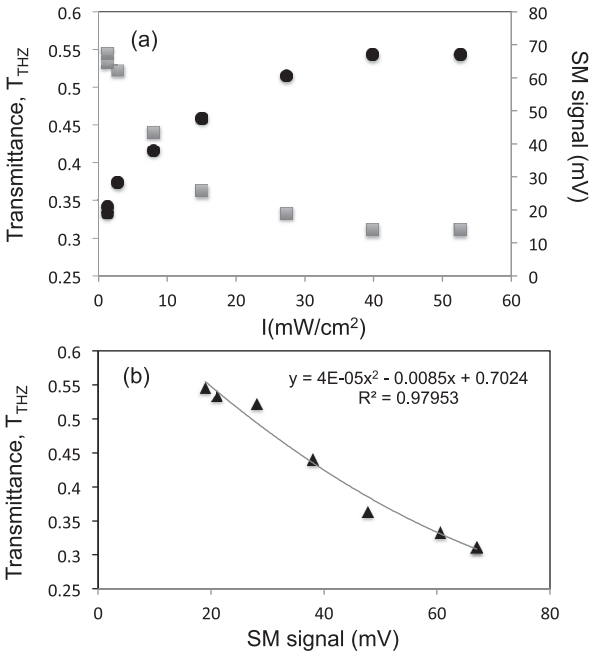

Fig. 2. – (a) Experimental estimation of of the THz transmittance (square symbol) and the SM signal (circle symbol) as a function of the NIR pump intensity. (b) Quadratic fit of the relation between the THz transmittance T_{THz} and the voltage modulation across the QCL terminals.

the semiconductor optical response is described by the Drude permittivity:

$$\epsilon(\omega^{\mathrm{THz}}) = \epsilon_\infty(\omega^{\mathrm{THz}}) - \sum_{j=e,h}\left(\frac{\omega_{p,j}^2\tau_j^2}{1+(\omega^{\mathrm{THz}}\tau_j)^2}\right) + i\sum_{j=e,h}\left(\frac{\omega_{p,j}^2\tau_j}{\omega^{\mathrm{THz}}(1+(\omega^{\mathrm{THz}}\tau_j)^2)}\right) = (n_r^{\mathrm{THz}} + n_i^{\mathrm{THz}})^2, \tag{3}$$

where $\epsilon_\infty(\omega^{\mathrm{THz}})$ is the background dielectric contribution, τ_e (τ_h) is the free electron (free holes) relaxation time. Finally the quantities n_r^{THz} and n_i^{THz} are the real and the imaginary part of complex refractive index n^{THz}. The plasma frequency $\omega_{p,e}$ ($\omega_{p,h}$) depends on the free electron N (hole P) density through the relation $\omega_{p,e} = (Nq^2/\epsilon_0 m_e^*)^{1/2}$ [$\omega_{p,h} = (Pq^2/\epsilon_0 m_h^*)^{1/2}$], where m_e^* (m_h^*) is the electron (hole) effective mass and q is the electron charge.

Using the Fresnel equations, the modulus of the external reflection coefficient R_{ext} at $z = 0$:

$$R_{\mathrm{ext}} = \frac{(1-n_r^{\mathrm{THz}})^2 + (n_i^{\mathrm{THz}})^2}{(1+n_r^{\mathrm{THz}})^2 + (n_i^{\mathrm{THz}})^2}. \tag{4}$$

Assuming that the photo-generated carriers are confined in a in a thin layer of length L_0 ($\approx 10\,\mu$m), the absorption length at ω^{IR}, the modulus of the THz transmission

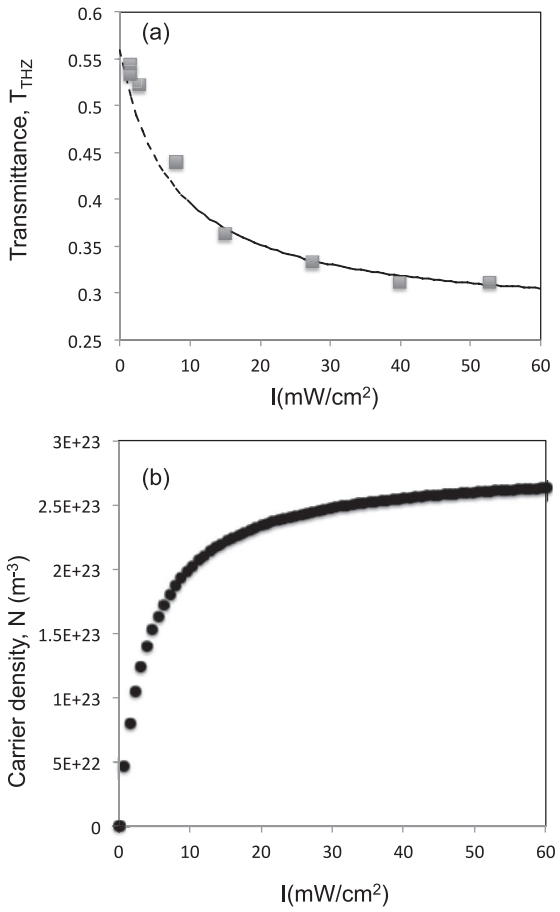

Fig. 3. – (a) Theoretical curve (dashed line) of the sample transmittance T_{THZ} as a function of the pump intensity I that best fits the experimental transmittance (squares symbols). (b) Free electrons density N corresponding to the theoretical transmittance in (a).

coefficient T_{THz}, which actually corresponds to the experimental transmittance shown in fig. 2(a), is

$$T_{\mathrm{THz}} = (1 - R_{\mathrm{ext}})e^{-\alpha L_0}e^{-\alpha' L}, \tag{5}$$

where $\alpha = 2\omega^{\mathrm{THz}} n_i^{\mathrm{THz}}/c$ and α' represent the absorption coefficients of the silicon sample in presence ($I \neq 0$) and in absence ($I = 0$) of NIR pumping respectively. Thus, according to eqs. (3)–(5), the optical response of the silicon slab at the THz wave can be easily tuned by photo-doping.

Figure 3(a) shows the transmittance T_{THz} estimated by using eq. (5) with the physical constants in table I and the values $N_0 = 3.0E + 23\,\mathrm{m}^{-3}$ and $I_{\mathrm{sat}} = 7\,\mathrm{mW/cm}^2$ that best fit the experimental transmittance shown in fig. 2(a). The corresponding carriers density N is reported in fig. 3(b). Finally, the relation between the measured SM signal in the THz QCL and the estimated free carrier density N is set trough the calibration curve in fig. 2(b).

TABLE I. – *Physical parameters* [13] *used in simulations.*

n_{IR}	$N^*(\mathrm{m}^{-3})$	$\tau_e(\mathrm{s})$	$\tau_h(\mathrm{s})$	ϵ_∞	m_e^*	m_h^*	$m_0(\mathrm{kg})$	$\alpha\prime(\mathrm{cm}^{-1})$
3.6	10^{18}	$2.3\,E-13$	$1.3\,E-13$	11.7	$0.27\,m_0$	$0.37\,m_0$	$9.11\,E-31$	2.5

5. – Free carriers imaging

In order to provide a proof of principle demonstration of carriers density imaging trough self-mixing in THz QCLs, the computer controlled SLM was used to project onto the silicon surface a series of NIR intensity pattern.

The spatially dependent SM signal was then acquired by a raster scanning of the pump area in the x-y plane (while keeping fixed the THz beam position) in order to map the spatially modulated distribution of the photo-generated carriers onto the semiconductor surface. A representative two-lobes beam profile is shown in fig. 4(a). The pump intensity was chosen to maximize the density of the photo-generated carriers in the illuminated area. The corresponding spatially modulated SM signal in fig. 4(b) well reproduces

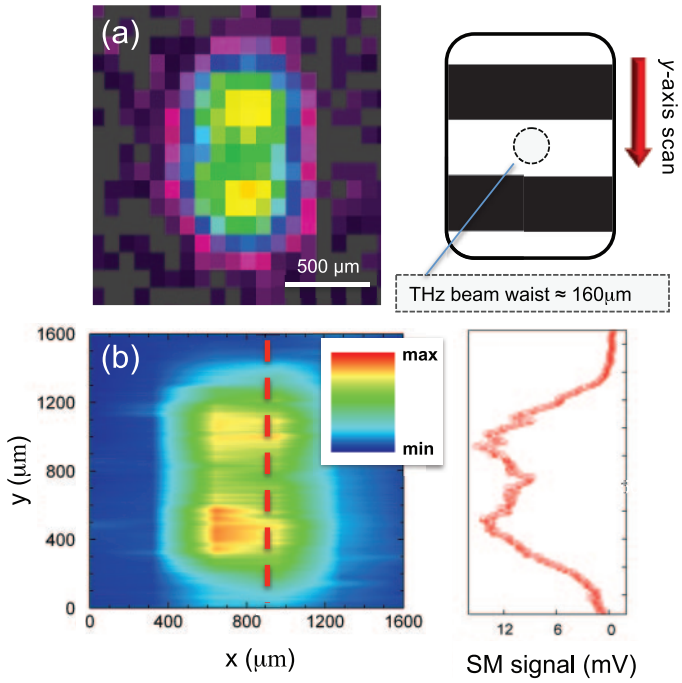

Fig. 4. – (a) Left: pump beam profile obtained wih a CCD replacing the silicon target. Right: sketch up of the imaging tecnique. The THz probe beam (beam waist $\approx 160\,\mu$m) is kept fixed during the raster scan of the pump beam along the x- and y-axis. Dark stripes denote the illuminated regions of the target. (b) Image plot of the SM signal obtained during the pump scanning. A representative section, as indicated by the dashed red line, is shown in the right panel. The minimum and maximum SM signal values corresponds to $N = N^* = 10^{18}\,\mathrm{m}^{-3}$ and $N = N_0 = 3.0E + 23\,\mathrm{m}^{-3}$ as obtained by fitting the SM signal with the theoretical prediction.

the pump intensity pattern. The associated distribution of the free electrons in the conduction band can be inferred by fitting the experimental data as described in the previous section. In the figure caption, the maximum and the minimum values of N is reported.

6. – Conclusions

In conclusion, an imaging technique of free carriers on a semiconductor surface based on a SM interferometry in a THz QCL was demonstrated. In a pump-probe experiment, a high reflectivity Tydex silicon sample was photo-doped with a spatially modulated NIR pump beam. The distribution of photo-generated carriers was inferred by probing the corresponding variation of the silicon target reflectivity with a THZ QCL in SM scheme. Thanks to the picosecond response time of QCLs, the proposed technique has the potential to map the spatio-temporal carriers dynamics in a wide class of optoelectronic devices.

* * *

The authors acknowledge partial financial support from MIUR PON02-0576 INNOVHEAD and MASSIME, PON01-02238 EURO6 and COST Action BM1205.

REFERENCES

[1] Kane D. M. and Shore K. A., *Optical feedback effects on semiconductor diode lasers*, in *Unlocking dynamical diversity* (Wiley J. and Sons) 2005.
[2] Rakic A. D. *et al.*, *Opt. Express*, **21** (2013) 22194.
[3] Dean P. *et al.*, *Appl. Phys. Lett.*, **103** (2013) 181112.
[4] Green R. P. *et al.*, *Appl. Phys. Lett.*, **92** (2008) 071106.
[5] Mezzapesa F. P. *et al.*, *Opt. Express*, **21** (2013) 13748.
[6] Schroder D. K., *Semiconductor Material and Device Characterization* (Wiley J. and Sons) 2006.
[7] Huber A. J. *et al.*, *Nano Lett.*, **8** (2008) 3766.
[8] Gabriel M. M. *et al.*, *Nano Lett.*, **13** (2013) 1336.
[9] Ulbricht R. *et al.*, *Rev. Mod. Phys.*, **83** (2011) 543.
[10] Mezzapesa F. P. *et al.*, *Appl. Phys. Lett.*, **104** (2014) 041112.
[11] Ashcroft N. W. and Mermin N. D., *Solid State Physics* (Holt, Rinehart, and Winston, New York) 1976.
[12] Garmine E. and Kost A., *Nonlinear Optics in Semiconductors I* (Academic Press) 1998.
[13] Riffe D. M., *J. Opt. Soc. Am. B*, **19** (2002) 121092.